Virchows Arch (2006) 449:348–357
DOI 10.1007/s00428-006-0258-6

ORIGINAL ARTICLE

Interstitial cells of Cajal could regenerate and restore their normal distribution after disrupted by intestinal transection and anastomosis in the adult guinea pigs

Feng Mei · Bin Yu · Hua Ma · Hong-jun Zhang · De-shan Zhou

Received: 31 March 2006 / Accepted: 16 June 2006 / Published online: 16 August 2006

Abstract Surgical manipulations of the gastrointestinal (GI) tract usually lead to loss of interstitial cells of Cajal (ICCs). The present study prepared to investigate whether ICCs can regenerate and restore their normal distribution up to 5 months after semitransection and end-to-end anastomosis of small intestines of adult guinea pigs. The segments of anastomosis were studied by immunohistochemistry with anti-KIT, 5-bromo-2′-deoxyuridine (BrdU), stem cell factor (SCF), and neurofilament 200 antibodies and also by transmission electron microscopy (TEM). At early stage, intestinal surgery led to intestinal wall impairment and ICCs loss, and ICCs near the site of anastomosis gradually increased in numbers. About 150 days postoperation, the distribution of ICCs and the microstructure of intestinal wall appeared to be similar with those of the control. By double immunostaining with BrdU and KIT antibodies, a number of proliferated ICCs were seen near the site of transection/anastomosis. Furthermore, KIT ligand, SCF, was mainly observed in the smooth muscle cells (SMCs), which are located close to ICCs. TEM observation revealed a number of immature and mature ICCs in this region. Our results indicated that ICCs could regenerate and restore their normal distribution after intestinal surgery and SMCs might be involved in the regenerated events of ICCs in the adult guinea pig GI tract.

F. Mei · B. Yu · H. Ma · H.-j. Zhang · D.-s. Zhou
Department of Histology and Embryology,
Third Military Medical University,
Chongqing 400038, People's Republic of China

D.-s. Zhou (✉)
Department of Histology and Embryology,
Capital University of Medical Sciences,
Beijing 100054, People's Republic of China
e-mail: dszhou2000@163.com

Keywords Interstitial cells of Cajal · KIT · Intestine · Abdominal surgery · C-kit

Abbreviations

DMP	Deep muscular plexus
GI	Gastrointestinal
ICCs	Interstitial cells of Cajal
IM	Intramuscular
MY	Myenteric plexus
SCF	Stem cell factor
SMCs	Smooth muscle cells

Introduction

Interstitial cells of Cajal (ICCs) are the pacemaker cells that generate and propagate the slow waves in alimentary tract, act as mediators of inputs from the enteric nervous system to gastrointestinal (GI) smooth muscles, and play an important role in the regulation of GI motility [8, 12, 16, 26]. Clinical studies indicate that ICCs are involved in some of GI motility disorders characterized by ICCs reduction and network impairment [4, 15]. Therefore, it was inferred that the deficiency of ICCs might contribute to the disappearance of slow waves and subsequent physical contraction of the smooth muscle in the GI tract [7, 23].

Surgical manipulations of the GI tract usually lead to postoperative GI dysmotilities (e.g., postoperative paralysis of intestine) in the clinic, and it often takes days or even months to recover depending on invasive degree [3]. Recent studies indicate that intestinal surgery results in

functional and morphological alterations of ICCs at the vicinity of the site of transection/anastomosis in the mouse small intestine, such as disappearance of both slow wave and c-kit receptor tyrosine kinase (KIT)-positive cells at 5 h after operation and the expression of KIT partial recovery at 24 h. These alterations of ICCs caused by operation are believed to be involved in short-term disruption of GI motor after surgery [30]. However, long-term alterations of ICCs at the site of transection/anastomosis after GI surgery and whether regeneration or degeneration of ICCs is involved in the recovery of the intestinal microstructure are still unknown. It was suggested that proliferation of ICCs could be detected only in embryonic and neonatal period, but whether ICCs could regenerate and restore their normal distribution after impairment in adult mammals remains essentially unsolved [9, 14, 20]. Therefore, the goal of our present study is to investigate the alterations of ICCs after they are disrupted by semitransection and anastomosis in small intestine of the adult guinea pigs up to 5 months. Immunohistochemical analyses and electron microscopy observation were performed on the specimens through the site of transection/anastomosis, including both oral and aboral ends. Our results indicated that ICCs could regenerate and restore their normal distribution after GI surgery and SMCs, which, expressing stem cell factor (SCF), might be involved in the regenerated events of ICCs.

Materials and methods

Animal treatment

Fifty guinea pigs (male or female, aged 6–8 weeks), purchased from Animal Center of Third Military Medical University (Chongqing, China), were used for intestinal surgeries in our experiments. The guinea pigs were anesthetized with pentobarbital sodium (Nembutal 50 μg/g); then approximately 30 mm of segment of ileum (100–150 mm from the ileocecal sphincter) was exposed; then the semitransection of the full thickness of intestinal the wall (both the longitudinal and circular muscle layer and mucosa) were cut down; and subsequent end-to-end seromuscular anastomosis were performed by using suture thread with 7-0 Ethilon. After absence of obstruction and leakage were confirmed, the abdomen was closed with 5-0 silk suture thread. Three sham-operated guinea pigs, which only underwent the laparotomy, were also prepared. Experimental animals were killed at 5, 10, 30, 50, 70 days and 3 and 5 months after operation by overdose anesthesia with pentobarbital. The experimental animals were performed in accordance with our University of Health Guide for the Care and Use of Laboratory Animals.

Immunohistochemistry

Small intestines that appeared normal in color and size from four animals for each group were used in present studies. Segments of small intestine, 10 mm in length from anastomosis to either end, were removed and opened along the mesenteric border. After enteric contents were washed away with phosphate-buffered saline (PBS), the specimens were quickly frozen with liquid nitrogen in optimal cutting temperature compound and the longitudinal sections through the site of anastomosis (6- to 8-μm-thick) were cut with a cryostat (Leica 1850) and were then fixed with 100% acetone for 15 min (4°C). Immunostaining procedures were done as previously described [10]. ICCs were identified by using a rat monoclonal antibody raised against KIT (ACK2, 5 μg/ml; eBioscience) and immunoreactivity was detected by using a fluorescein isothiocyanate-conjugated secondary antibody (anti-rat IgG, 1:150; Jackson ImmunoResearch Lab) or peroxidase-conjugated secondary antibody (anti-rat IgG, 1:100; DAKO), and horseradish peroxidase reaction was developed in a solution containing 0.05% of 3,3′-diaminobenzidine tetrahydrochloride (DAB; Sigma) in 0.05 M Tris–HCl buffer (pH 7.6) with 0.3% H_2O_2 and the sections were counterstained with hematoxylin after immunohistochemical staining. Detection of SCF or nerve with a mouse monoclonal antibody raised against SCF (5 μg/ml; Santa Cruz, USA) or neurofilament 200 (NF200, 1:100; Boster), respectively, was carried out with the same procedures as described above. The SCF or NF200 positive cells were examined by Cy3-conjugated secondary antibody (anti-mouse IgG, 1:200; Sigma). Control specimens were prepared in a similar manner, but each primary antibody in the incubation solution was omitted. The stained results were examined with a BX51 fluorescence microscope (OLYMPUS, Japan) with an excitation wavelength appropriate for fluorescein isothiocyanate (488 nm) or Cy3 (552 nm).

Detection of regenerated interstitial cells of Cajal

To identify cell proliferation, 5-bromo-2′-deoxyuridine (BrdU, 13 μg/g every 2 days; Sigma) was injected intraperitoneally for three animals of each operated group, i.e., 5-, 10-, 30-, and 50-day groups and nonoperated group until the day before they were killed. For detection of regenerated ICCs, KIT immunocytochemical staining with ACK2 was first carried out as described above and then the stained sections were further fixed in 4% paraformaldehyde in 0.1 M PB at pH 7.2 for 30 min, Baker's solution for 10 min, and 1% glutaraldehyde in the same buffer for 15 min in turn. After rinsing in PBS, the specimens were pretreated with pepsin (0.006%; Sigma) for 30 min at 37°C, followed by partial denaturation of double-stranded DNA

with 4 N HCl for 30 min at 37°C. To reveal BrdU, the sections were incubated with a mouse monoclonal antibody raised against BrdU (3 μg/ml; DAKO) overnight at 4°C and then with Cy3-conjugated secondary antibody (anti-mouse IgG, 1:200; Sigma) for 1 h at 25°C.

Measurement and statistical analysis

Twenty sections were sampled from 100 series of sections of each animal in a systematic random manner. In practice, every fifth section was systematically sampled, the first one being randomly sampled from the first five sections. BrdU/KIT-positive cells within both oral and aboral anastomotic ends were counted. Data were expressed as means±SEM. Differences in the data were evaluated by single factor analysis of variance. $P<0.05$ was taken as a statistically significant difference. The *N* values reported in the text referred to the number of animals in which BrdU injection was performed on. The numbers of KIT/BrdU double positive cells within anastomotic region at different time and different locations, including myenteric plexus (MY), deep muscular plexus (DMP) and intramuscular (IM), were measured and analyzed.

Transmission electron microscopy

According to immunostaining results, the samples from three animals of 70 days postoperative group were performed for the ultrastructural observation. In brief, the pieces of anastomotic region were placed in a fixative made of 2.5% glutaraldehyde and 4% paraformaldehyde in 0.1 M PB at pH 7.2 for 2 h at 4°C. The specimens were washed in the same buffer and subsequently postfixed with 1% osmium tetroxide (OsO_4) in the same buffer for 1 h at 4°C. After osmication, the specimens were rinsed in distilled water and then block-stained with a saturated aqueous uranyl acetate solution for 2 h, dehydrated through a graded series of alcohols, and embedded in Epon 812 resin (TAAB, England). Ultrathin sections were cut using a Reichert ultramicrotome and double-stained with uranyl acetate and lead citrate and observed with Philips Tecnai 10 transmission electron microscope.

Results

On the longitudinal sections through the site of the surgical incision with hematoxylin and eosin staining, the full thickness of the intestinal wall were broken down and each anastomotic end was divided into three areas. The cut ends of intestinal smooth muscle layers were taken as area I, which appeared to be thicker than the normal state for smooth-muscle contraction. Adjacent to this area, where suturation was performed, the muscle layers seemed to be thinner because of sutural tension (area II), while area III, between the oral and aboral ends of serosal surfaces in the anastomosis, showed a triangle-like area (Fig. 1a).

The alterations of distribution of interstitial cells of Cajal in postoperation intestines

In normal and sham-operated animals, many ICCs and their cytoplastic processes forming the networks were usually seen at the MY level, associated with DMP and IM. Five and 10 days postoperation, the longitudinal sections showed that smooth muscle layers and ICCs cellular networks in area I were disrupted by surgery, and IC-MY and IC-DMP were mostly lost in area II, while area III and the site of surgical incision were mainly filled with a large amount of connective tissue where no ICCs-like cells were seen (Fig. 1b). From 10 to 30 days after operation, some ICCs-like cells showed up in areas I, II, and III. Those cells were characterized by oval-shaped nuclei with poor cytoplasm and 1–2 short and thin processes, but they were still irregularly distributed in above areas (Fig. 1c,d). Around 50 days postoperation, the distribution of ICCs-like cells and microstructure of intestinal wall in areas I and II were of partial recovery. On the longitudinal sections, IC-MY and IC-DMP could be distinguishable and their processes were prolonging toward another cut end (Fig. 1e). In 70 days postoperation, the intestinal wall of areas I and II tended to restore normal microstructure, besides the density of IC-MY and IC-DMP was still increased (Fig. 1f), and ICCs-like cells with 2–3 thin processes began to appear in area III (Fig. 1g). In 90 days, the distribution of ICCs in areas I and II tended to restore to normal, but not interconnected yet. About 5 months after operation, along with the recovery of smooth muscle layers, oral and aboral anastomotic ends were interconnected and ICCs-like cells were also redistributed to continue with IC-MY and IC-DMP, respectively (Fig. 1h).

Identification of regenerated interstitial cells of Cajal

Although we observed that ICCs could restore their normal distribution after surgery, it was not clear if regeneration or proliferation of ICCs were involved in this process. Therefore BrdU incorporation was used and double immunostaining with anti-BrdU monoclonal antibody and anti-KIT monoclonal antibody was employed. Only KIT/BrdU double labeling cells with processes were considered as proliferated ICCs. No KIT/BrdU double labeling cells were observed in the intestinal wall of the control and 5 days postoperation of animals, while a large amount of intestinal epithelial cells (Fig. 2a) and some fibroblasts and smooth muscle cells (SMCs) were often incorporated by

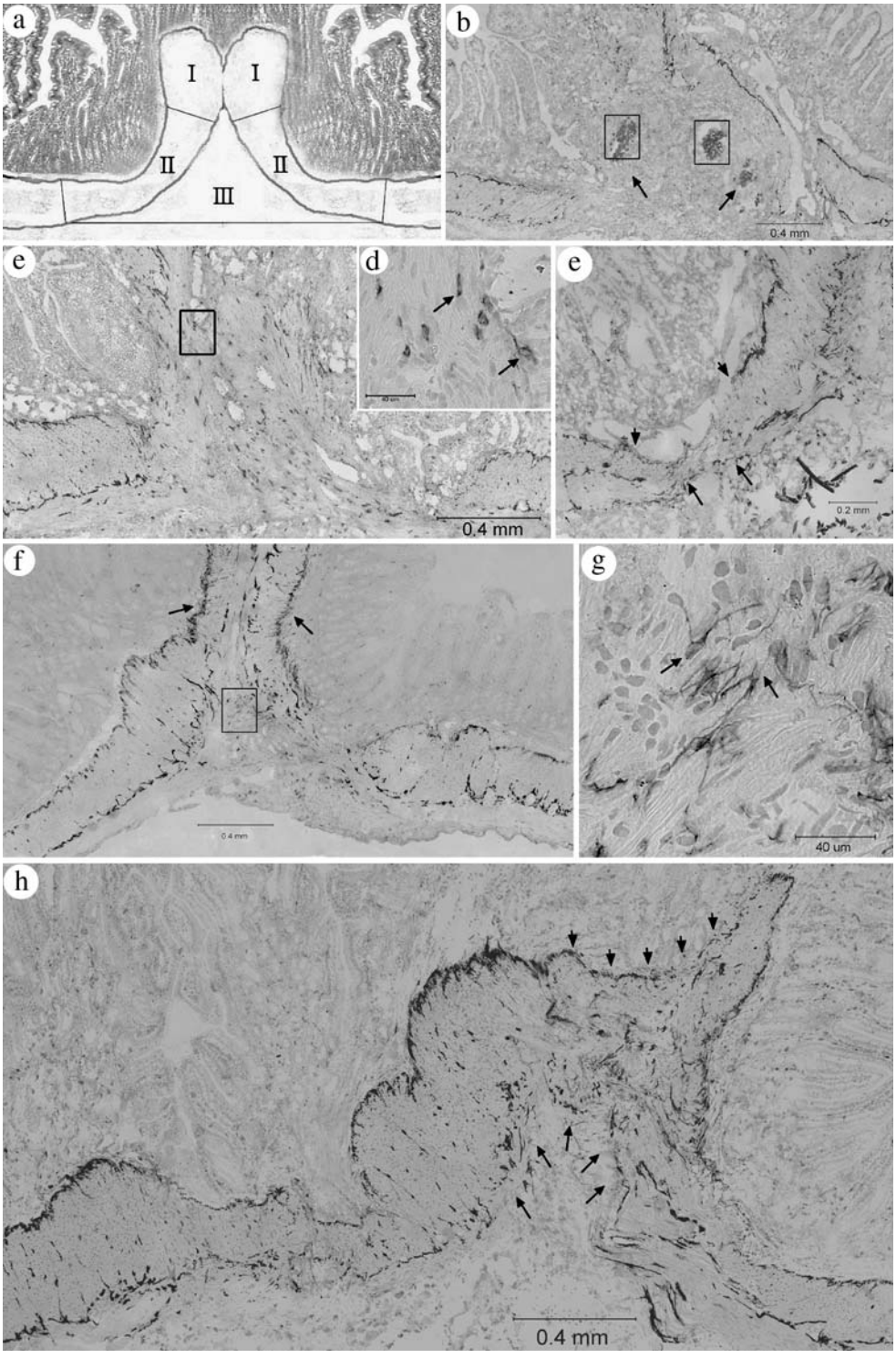

Fig. 1 Longitudinal sections showing alterations of ICCs from 10 to 150 days postoperation with KIT immunohistochemical staining. **a** The rough sketch displaying the three areas of anastomosis: *area I* is the cut ends of intestinal smooth muscle layers; *area II* is the place where suturation was performed; and *area III* is between oral and aboral serosal surface of anastomotic ends that showed a *triangle*-like area. **b** KIT-positive cells in *areas I* and *II* were disrupted and partly lost (*arrows*) 10 days postoperation (*frames* showing suture thread). **c** Some ICCs-like cells irregularly showed up in the three areas at 30 days postoperation. **d** Higher magnification of ICCs-like cells (*arrows*) in *area III* (*frame* in subpanel **c**). **e** ICCs-like cells increased in *areas I*, *II*, and *III* and showed a tendency to form IC-MY (*arrows*) and IC-DMP (*arrowheads*) at 50 days postoperation. **f** IC-DMP and IC-MY in *areas I* and *II* were still increased in density at 70 days (*arrows*) postoperation. **g** Higher magnification showing ICCs-like cells in *area III* with 2–3 slender processes and branches (*arrows*) (*frame* in subpanel **f**). **h** One hundred and fifty days postoperation, oral and aboral anastomotic ends including IC-MY (*arrows*) and IC-DMP (*arrow heads*) that are interconnected. *Scale bar* **b**, **c**, **f**, and **h**=0.4 mm; **d**, **g**=40 μm; and **e**=0.2 mm

BrdU at these animals. Ten-day postoperation, 0~3 (n=3, average 1.48±1.19) KIT/BrdU double staining cells were observed in each oral or aboral anastomotic end, and these cells were mainly seen in the DMP (74%) region or MY (23%) and seldom within smooth muscle layers (3%). It should be noticed that no KIT/BrdU double staining cells were observed in the area that was beyond 2.1 mm from the site of anastomosis. The number of KIT/BrdU double staining cells was gradually increased to 6–10 (n=3, averaged 7.9±2.4) around 30 days after operation. Among them, about 62% were located at the DMP region with enriched cytoplasm and oval-shaped nuclei, and some located around MY (26%) and within smooth muscle layers (12%). Most of them (95%) were distributed within 4.0 mm from anastomotic site to the oral or aboral end (Fig. 2b). Fifty days after operation the number of KIT/

BrdU double staining cells were increased to 14~18 (n=3, average 16.47±1.98). Those cells were nearly located within 6.5 mm from anastomotic site to the oral or aboral end. Among them, 58% were distributed in the places of DMP, 25% in the MY with 2~3 thin and long processes and 17% in the smooth muscle layers (Fig. 2c,d). The statistical analysis showed that the number of regenerated/proliferated ICCs at various times and locations were significantly different (P<0.05), whereas they have no significant difference between the oral and aboral ends of the anastomosis (P>0.05) (Fig. 3a,b).

Stem cell factor, smooth muscle, and nerves in the anastomotic intestinal wall

Previous studies have demonstrated that the KIT-SCF signal pathway is essential to the development and survival of ICCs [13, 24]. To explore the possible roles of the signal pathway during ICCs regeneration, double immunostaining with anti-SCF and anti-KIT antibodies were performed. Strong SCF immunoreactions were mainly observed in SMCs, including the circular and longitudinal SMCs, and weak in neurons of MY, while no SCF immunoreaction was visible in the connective tissue cells (Fig. 4a). By the SCF immunostaining, we found that the longitudinal SMCs began to grow from area II to area III and then toward the opposite side around 30 days postoperation and completely interconnected in about 70 days (Fig. 4b,c). In contrast, the circular smooth muscle layer at the site of the anastomosis did not completely interconnect until 5 months (Fig. 4d). It was noticed that increased ICCs were in higher density and only distributed among SCF-positive SMCs in the region of anastomosis and in area III (Fig. 4e); ICCs were also observed around or within out-growing SMC bundles from area II (Fig. 4f). Meanwhile, immunostaining with anti-NF200 showed that the MY and DMP were also disrupted and they began to regrow out within SMCs 30 days postoperation (data not shown). They were

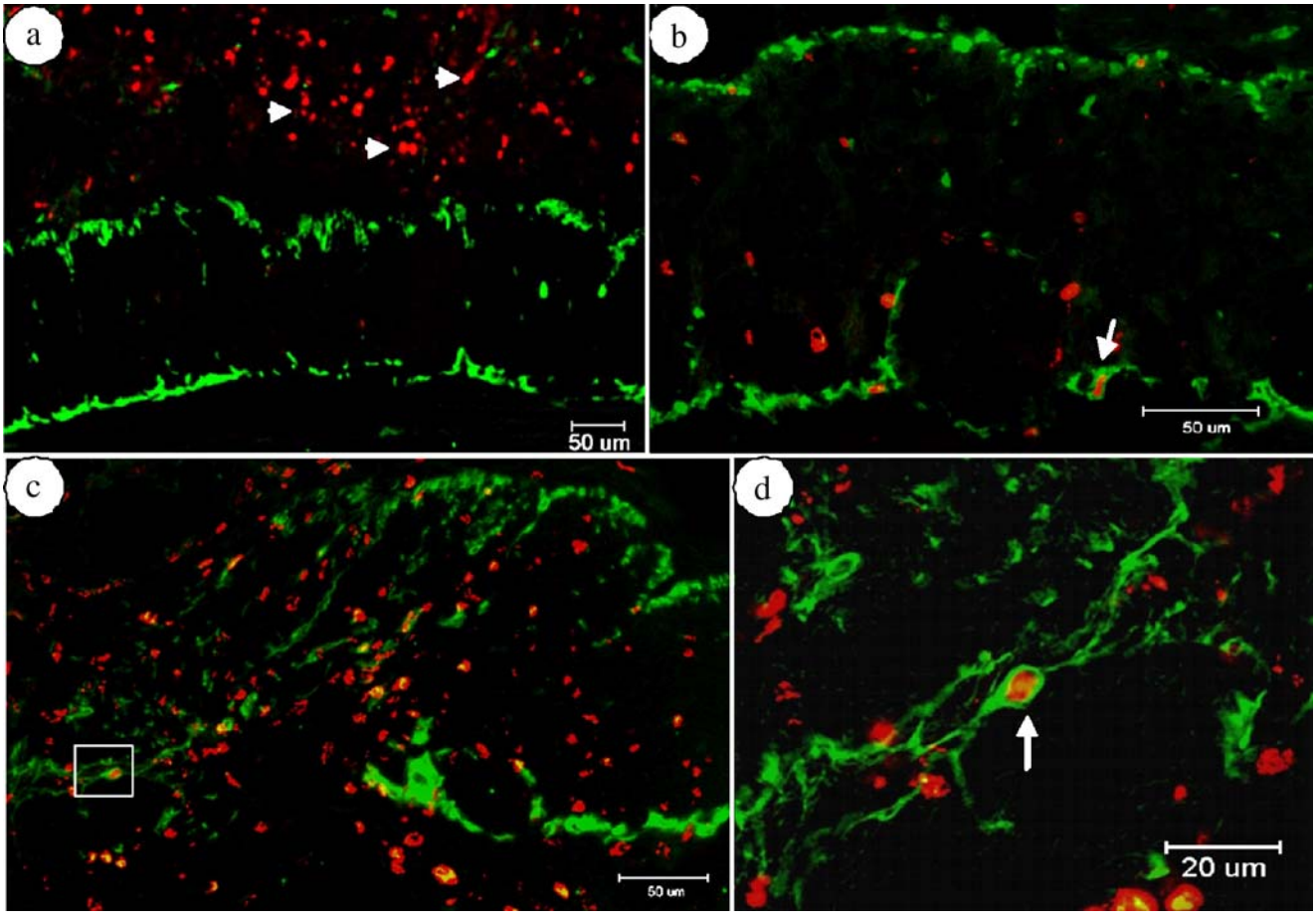

Fig. 2 KIT (*green*)/BrdU (*red*) double staining showing regenerated ICCs. **a** No KIT/BrdU double-staining cells were observed on the longitudinal sections of the control group, while a large number of epithelial cells in the intestine were BrdU-positive (*arrowheads*). **b** KIT/BrdU double-staining cells, as proliferated ICCs, were seen in normal intestinal wall adjacent to anastomosis at 30 days post-operation (*arrow*). **c** Proliferated ICCs were often detected in the site of anastomosis at 50 days postoperation. **d** Higher magnification showing KIT/BrdU double-labeling cells with slender processes (*frame* in subpanel **c**). *Scale bar* **a**–**c**=50 μm; **d**=20 μm

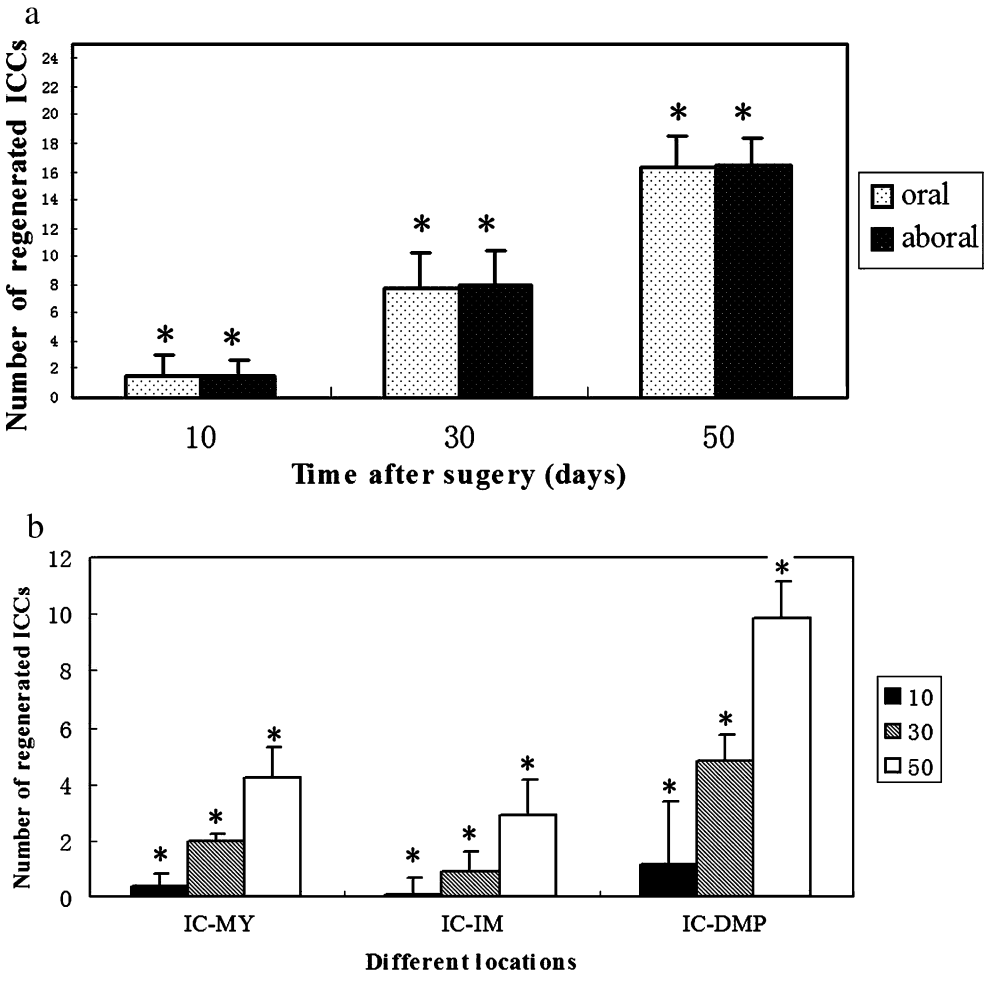

Fig. 3 Account of the number of KIT/BrdU double-staining cells at different time and locations. Each histogram represents the means±SEM. **a** The number of regenerated ICCs was gradually increased from 10-, 30- and 50-day groups of postoperation (*P<0.05). The number of regenerated ICCs was similar between oral and aboral (P>0.05) in each group. **b** The amounts of KIT/BrdU double-staining cells in MY, IM, and DMP regions were significantly different (*P<0.05)

redistributed to continue with MY and DMP at the anastomotic region at 5 months postoperation (Fig. 4g).

Ultrastructural features of the region of anastomosis

As mentioned above, 70 days postoperation animals appeared to be in the middle of the process, so the ultrastructural features of these samples were selectively studied by transmission electron microscopy (TEM). The region of anastomosis was filled with abundant collagen fibers, fibroblasts (Fig. 5a), and some SMCs (Fig. 5b) and a number of mature and immature ICC-like cells were also often seen in this region. The whole ICCs shape including cell bodies and long processes can hardly be viewed in a single profile because ICCs have slender processes. In an ultrathin section, the mature ICCs seemed to be characterized by the presence of many mitochondria, well-developed smooth endoplasmic reticulum, and microtubules (Fig. 5c). However, in the atypical ICCs, immature ones, were characterized by the presence of abundant cytoplasm with numerous free ribosomes, which were essential to the synthesis of structural protein for the cells (Fig. 5d).

Discussion

Clinical and experimental studies have suggested that loss of ICCs are associated with intestinal motor dysfunction and that GI surgeries inevitably lead to loss of ICCs and network impairment [16]. The present study established an animal model and demonstrated that IC-MY and IC-DMP were disrupted, and ICCs were partly lost in anastomotic region 5 days postoperation. These alterations might result from surgical manipulation (e.g., transection or anastomosis), sutural tension, local inflammatory reactions [6], and KIT phenotype loss in parts of ICCs [5]. We found that ICCs-like cells and processes in areas I and II were gradually increased with the increase of time and recovered to normal distribution around 70 days after GI surgery, but were not yet rejoined in area III. It appeared that at 150 days postoperation, the microstructure of the intestinal wall nearly restored to the same as those of the control group, such as ICCs, SMCs, and nerve fibers growing through the site of anastomosis. It was surprising that the distribution of ICCs and the microstructure of the intestinal wall took nearly 5 months to recover. However, we did not

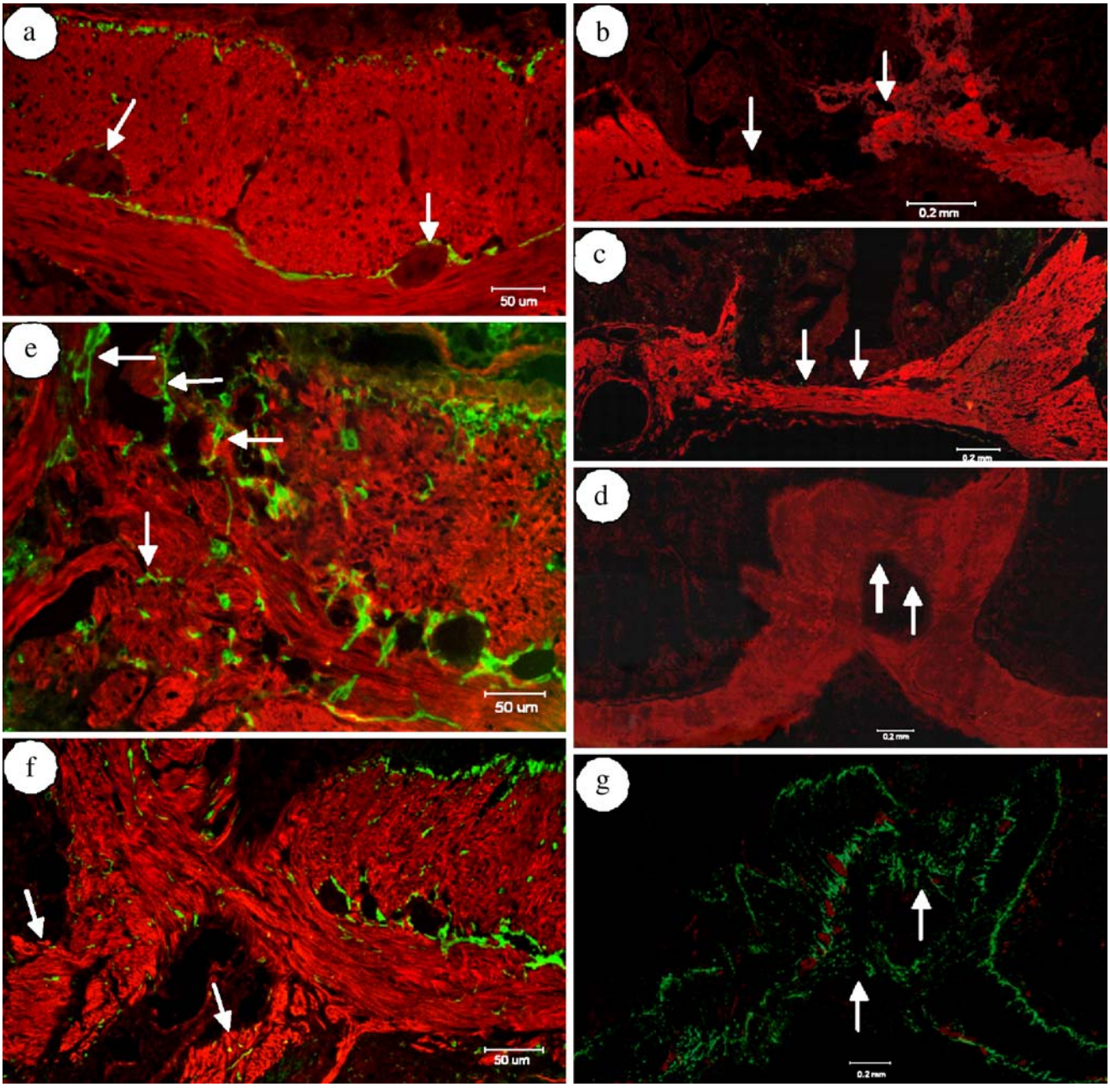

Fig. 4 **a**–**f** KIT(*green*)/SCF(*red*) double staining of the operated intestine. **a** SCF was mainly expressed in SMCs and weakly in neurons (*arrows*). **b**, **c** Longitudinal smooth muscle layer began to grow at 30 days postoperation (*arrows*) (subpanel **b**) and interconnected at 70 days (*arrows*; subpanel **c**). **d** Circular smooth muscle layer interconnected 150 days postoperation (*arrows*). **e** The density of ICC-like cells was higher among the SCF-positive SMCs in the site of anastomosis (*arrows*). **f** In *area III*, ICCs-like cells showed a tendency of outgrowth with SMCs bundles at anastomosis (*arrows*). **g** ACK2 (*green*)/NF200 (*red*) double staining showing that ICCs and nerves reconnected 150 days after surgery and also showing smooth muscle layers (*arrows*). *Scale bar* **a**, **e**, and **f**=50 μm; **b**–**d**, and **g**=0.2 mm

observe any symptoms of GI motility dysfunctions (e.g., vomiting or diarrhea) on our experimental animals, and dysfunction of GI motility after abdominal surgical manipulation usually would not last for such a long time in clinic [1, 21, 22]. The possible interpretations might be the following: (1) ICCs and the enteric nervous system adjacent to anastomosis (>2.4 mm) still kept normal distribution that might compensate the disabled segment of the intestine or operated site; and (2) The anastomotic region is covered by a connective tissue, which might prevent from overdistension, infection, and leakage, and support the transportation of the GI movement. Our results would help clinical surgeons understand prolonged inhibition of bowel motility functions, which often occurred in some patients with GI

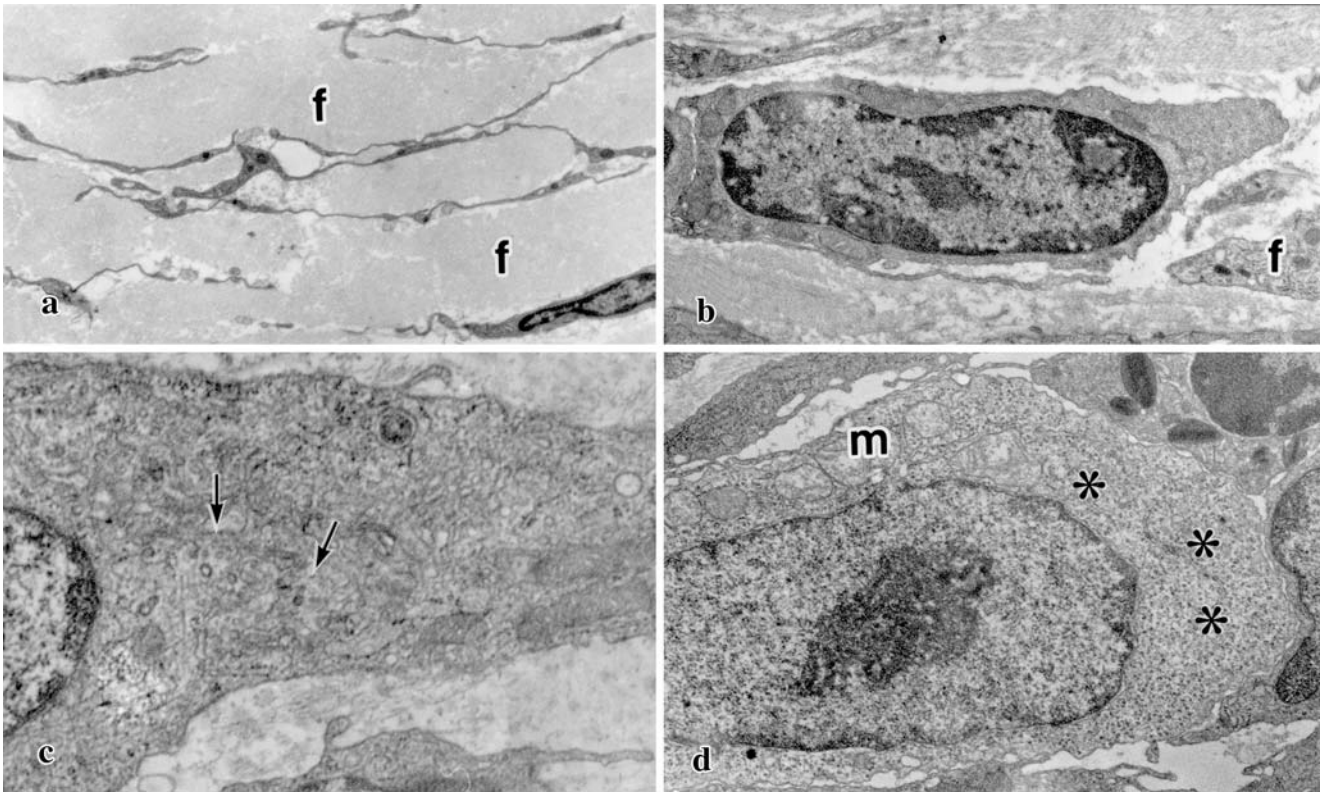

Fig. 5 Electron micrographs showing the region of anastomosis at 70 days postoperation. **a** Low-magnification micrograph of abundant collagen fibers (*f*) and partial processes of the fibroblasts (×4,200). **b** SMC with a number of mitochondria and abundant sarcoplasm was also observed at vicinity of anastomosis (×5,200). **c** A mature ICC-like cell with abundant cytoplasm, smooth endoplasmic reticulum, and a large number of microtubules were seen in the site of anastomosis (×9,000). **d** One of the immature ICC-like cell characterized by the presence of a large amount of free ribosomes (×11,000)

operations. Those might be related to the fact that ICCs were lost in a large amount and took a long time to restore to their normal distribution. Moreover, it was reported that distention and inflammatory factors after GI surgeries might produce a regional pseudoobstruction that might lead to further loss of ICCs and contribute to a longer motility disorders in clinic [1].

Previous studies have demonstrated that ICCs originated from mesenchymal cells [9, 11], and the proliferation of ICCs and extension of the processes are only observed in embryonic and neonatal periods in mammals, and even ICCs, which derive from 6-day neonatal mice, could not increase in number in culture [14, 27], indicating that the proliferation of ICCs depend on the age in vitro. However, after sequential injection of BrdU for 2 weeks, no KIT/BrdU double labeling cells were observed in adult guinea pigs, which hinted that ICCs might have a low renewal rate in the normal condition. Therefore, this animal model was also used to investigate the regenerated events and our results revealed that KIT/BrdU double labeling cells, the proliferated ICCs, were observed 10 days postoperation. The amount of these cells at 50 days postoperation rose about nine times as many as it was at 10 days. They were mainly found in the site of anastomosis and within the intact networks adjacent to this region, while no KIT/BrdU double labeling cells were seen in the control and sham-operated groups. TEM observation also revealed a number of immature ICC-like cells in the regions of anastomosis. All together, our results indicated that ICCs in the adult GI tract still possessed the ability to regenerate in the condition of lost ICCs. However, according to our data, it was not clear that the regenerated ICCs originated from residual ICCs or precursor/stem cells. Basing on morphological features and locations of KIT/BrdU double labeling cells, it was suggested that proliferation of the residual ICCs near the site of anastomosis might be one of the resources, meanwhile mesenchymal stem cells, the precursor of both ICCs and SMCs, could not be excluded [28].

With regard to the factors that might be involved in the proliferation of ICCs, SCF, the ligand of KIT receptor, is considered because KIT–SCF signal pathway plays an important role in the development and survival of ICCs [2, 13]. It has been demonstrated that mutation of c-kit or steel or blockage of KIT–SCF signal pathway with antibody against KIT would lead to the disappearance of ICCs and slow waves and result in distention and paralysis of

intestine [18, 23, 24]. In the present study, the expression of SCF and KIT were measured by double immunostaining, SCF immunoreactions were mainly found in SMCs, and ICCs were nearly in the vicinity of SCF-positive SMCs and among the SMCs bundles, which grew out from area II to area III. These results suggested that SMCs, which are expressing SCF, might be involved in the regenerated events of ICCs after GI surgery. This is coincident with other reports that SMCs alone could provide a suitable microenvironment for the survival of ICCs via expressing SCF [11, 29, 31]. Moreover, besides SMCs, nerves are closely related with ICCs morphologically and physiologically, although it was demonstrated that neither neurons nor glial cells are necessary for the development or survival of ICCs [19, 32] and the expression of SCF in SMCs appears to be sufficient to stimulate growth of ICCs and formation of the cellular network [17, 25]. Furthermore, it appeared that nerve fibers and neurons were not likely to locate to ICCs as tightly as SMCs and expressed SCF weakly in our experiments, but their contributions during the restoration should be carefully studied in the further researches.

In conclusion, our results indicated that ICCs could regenerate and their processes could extend gradually toward the site of anastomosis after being disrupted by intestinal semitransection and anastomosis and finally restore their normal distribution in the adult guinea pigs. SMCs, which are expressing SCF, might be one of the factors that were involved in the regenerated events of ICCs. These results might provide a clue to the understanding and clinical treatment of GI motility disorders.

Acknowledgements We thank Dr. Y. Tang (Department of Histology and Embryology, Chongqing University of Medical Sciences) for critical reading the manuscript. This work was supported in parts by grants no. 30470911 and 30570983 from the National Science Foundation of China (NSFC). Feng Mei and Bin Yu contributed equally to this work.

References

1. Baig MK, Wexner SD (2004) Postoperative ileus: a review. Dis Colon Rectum 47:516–526
2. Beckett EA, Horiguchi K, Khoyi M, Sanders KM, Ward SM (2002) Loss of enteric motor neurotransmission in the gastric fundus of Sl/Sl(d) mice. J Physiol 543:871–887
3. Behm B, Stollman N (2003) Postoperative ileus: etiologies and interventions. Clin Gastroenterol Hepatol 1:71–80
4. Bharucha AE, Philips SF (2001) Slow-transit constipation. Curr Treat Options Gastroenterol 4:309–315
5. Chang IY, Glasgow NJ, Takayama I, Horiguchi K, Sanders KM, Ward SM (2001) Loss of interstitial cells of Cajal and development of electrical dysfunction in murine small bowel obstruction. J Physiol 536:555–568
6. Faussone-Pellegrini MS, Gay J, Vannucchi MG, Corsani L, Fioramonti J (2002) Alterations of neurokinin receptors and interstitial cells of Cajal during and after jejunal inflammation induced by Nippostrongylus brasiliensis in the rat. Neurogastroenterol Motil 14:83–95
7. Isozaki K, Hirota S, Miyagawa J, Taniguchi M, Shinomura Y, Matsuzawa Y (1997) Deficiency of c-kit+ cells in patients with a myopathic form of chronic idiopathic intestinal pseudo-obstruction. Am J Gastroenterol 92:332–334
8. Kito Y, Ward SM, Sanders KM (2005) Pacemaker potentials generated by interstitial cells of Cajal in the murine intestine. Am J Physiol Cell Physiol 288:C710–C720
9. Kluppel M, Huizinga JD, Malysz J, Bernstein A (1998) Developmental origin and Kit-dependent development of the interstitial cells of Cajal in the mammalian small intestine. Dev Dyn 211:60–71
10. Komuro T, Zhou DS (1996) Anti-c-kit protein immunoreactive cells corresponding to the interstitial cells of Cajal in the guinea-pig small intestine. J Auton Nerv Syst 61:169–174
11. Lecoin L, Gabella G, Le Douarin N (1996) Origin of the c-kit-positive interstitial cells in the avian bowel. Development 122:725–733
12. Liu LW, Thuneberg L, Huizinga JD (1998) Development of pacemaker activity and interstitial cells of Cajal in the neonatal mouse small intestine. Dev Dyn 213:271–282
13. Mikkelsen HB, Malysz J, Huizinga JD, Thuneberg L (1998) Action potential generation, kit receptor immunohistochemistry and morphology of steel-Dickie (Sl/Sld) mutant mouse small intestine. Neurogastroenterol Motil 10:11–26
14. Nakahara M, Isozaki K, Vanderwinden JM, Shinomura Y, Kitamura Y, Hirota S, Matsuzawa Y (2002) Dose-dependent and time-limited proliferation of cultured murine interstitial cells of Cajal in response to stem cell factor. Life Sci 70:2367–2376
15. Rolle U, Piotrowska AP, Nemeth L, Puri P (2002) Altered distribution of interstitial cells of Cajal in Hirschsprung disease. Arch Pathol Lab Med 126:928–933
16. Sanders KM, Ordog T, Koh SD, Torihashi S, Ward SM (1999) Development and plasticity of interstitial cells of Cajal. Neurogastroenterol Motil 11:311–338
17. Sanders KM, Ordog T, Ward SM (2002) Physiology and pathophysiology of the interstitial cells of Cajal: from bench to bedside. IV. Genetic and animal models of GI motility disorders caused by loss of interstitial cells of Cajal. Am J Physiol Gastrointest Liver Physiol 282:G747–G756
18. Torihashi S, Ward SM, Nishikawa S, Nishi K, Kobayashi S, Sanders KM (1995) c-kit-dependent development of interstitial cells and electrical activity in the murine gastrointestinal tract. Cell Tissue Res 280:97–111
19. Torihashi S, Yoshida H, Nishikawa S, Kunisada T, Sanders KM (1996) Enteric neurons express steel factor-lacZ transgene in the murine gastrointestinal tract. Brain Res 738:323–328
20. Torihashi S, Ward SM, Sanders KM (1997) Development of c-Kit-positive cells and the onset of electrical rhythmicity in murine small intestine. Gastroenterology 112:144–155
21. Tsukamoto K, Mizutani M, Yamano M, Tagi Y, Takeda M (2000) The effect of SK-896 on post-operative ileus in dogs: gastrointestinal motility pattern and transit. Eur J Pharmacol 401:97–107
22. van der Velden MA, Klein WR (1993) The effects of cisapride on the restoration of gut motility after surgery of the small intestine in horses; a clinical trial. Vet Q 15:175–179
23. Ward SM, Burns AJ, Torihashi S, Sanders KM (1994) Mutation of the proto-oncogene c-kit blocks development of interstitial cells and electrical rhythmicity in murine intestine. J Physiol 480(Pt 1): 91–97
24. Ward SM, Burns AJ, Torihashi S, Harney SC, Sanders KM (1995) Impaired development of interstitial cells and intestinal electrical rhythmicity in steel mutants. Am J Physiol 269: C1577–C1585

25. Ward SM, Ordog T, Bayguinov JR, Horowitz B, Epperson A, Shen L, Westphal H, Sanders KM (1999) Development of interstitial cells of Cajal and pacemaking in mice lacking enteric nerves. Gastroenterology 117:584–594
26. Ward SM, Beckett EA, Wang X, Baker F, Khoyi M, Sanders KM (2000) Interstitial cells of Cajal mediate cholinergic neurotransmission from enteric motor neurons. J Neurosci 20:1393–1403
27. Wester T, Eriksson L, Olsson Y, Olsen L (1999) Interstitial cells of Cajal in the human fetal small bowel as shown by c-kit immunohistochemistry. Gut 44:65–71
28. Wu JJ, Rothman TP, Gershon MD (2000) Development of the interstitial cell of Cajal: origin, kit dependence and neuronal and nonneuronal sources of kit ligand. J Neurosci Res 59:384–401
29. Yamataka A, Kato Y, Tibboel D, Murata Y, Sueyoshi N, Fujimoto T, Nishiye H, Miyano T (1995) A lack of intestinal pacemaker (c-kit) in aganglionic bowel of patients with Hirschsprung's disease. J Pediatr Surg 30:441–444
30. Yanagida H, Yanase H, Sanders KM, Ward SM (2004) Intestinal surgical resection disrupts electrical rhythmicity, neural responses, and interstitial cell networks. Gastroenterology 127:1748–1759
31. Young HM, Ciampoli D, Southwell BR, Newgreen DF (1996) Origin of interstitial cells of Cajal in the mouse intestine. Dev Biol 180:97–107
32. Young HM, Torihashi S, Ciampoli D, Sanders KM (1998) Identification of neurons that express stem cell factor in the mouse small intestine. Gastroenterology 115:898–908